Applied Catalysis B: Environmental 123–124 (2012) 433–439

Contents lists available at SciVerse ScienceDirect

Applied Catalysis B: Environmental

journal homepage: www.elsevier.com/locate/apcatb

Remediation of 2,4-dichlorophenol contaminated water by visible light-enhanced WO_3 photoelectrocatalysis

E.O. Scott-Emuakpor[a,b], A. Kruth[c], M.J. Todd[b], A. Raab[b], G.I. Paton[a], D.E. Macphee[b,*]

[a] Institute of Biological & Environmental Sciences, Cruickshank Building, University of Aberdeen, St. Machar Drive, Aberdeen AB24 3UU, UK
[b] School of Natural and Computing Sciences, University of Aberdeen, Meston Walk, Aberdeen AB24 3UE, UK
[c] Leibniz Institute for Plasma Science and Technology, Felix-Hausdorff-Str. 2, 17489 Greifswald, Germany

ARTICLE INFO

Article history:
Received 11 January 2012
Received in revised form 7 May 2012
Accepted 9 May 2012
Available online 15 May 2012

Keywords:
Tungsten trioxide
2,4-Dichlorophenol
Photoelectrocatalysis
Waste water
Bacterial biosensor

ABSTRACT

The application of semiconductor photocatalysis in waste water treatment has been intensively investigated over the past decade. Most studies involve titanium-based photocatalysts; however, practical applications are still limited by their poor visible light activity. As an alternative, a tungsten trioxide-based photoelectrocatalytic fuel cell (PECFC) with a cell configuration based on the proton exchange membrane fuel cell (PEMFC) technology has been employed for pollutant remediation. In this study, the degradation of a persistent chlorophenol (2,4-dichlorophenol) was assessed using a visible light active tungsten trioxide photocatalyst. The degradative progress of the 2,4-DCP was monitored over a period of 24 h by both chemical analysis and a bacterial biosensor (*Escherichia coli* HB101 pUCD607) toxicity assay. A 74% decrease in concentration of the 2,4-DCP was observed after a period of 24 h, from which *ca.* 54% were accountable to degradation processes and 20% due to pollutant losses by adsorption or volatilisation. The biosensor toxicity response correlated well with the observed concentration reduction of 2,4-DCP, but also indicated the formation of more toxic intermediates. HPLC–MS analysis was carried out to study intermediate degradation products. There were indications of the occurrence of stable dimers within the first few hours of the degradation process and the formation of intermediate degradation products of higher bacterial toxicity than the parent compound. Although the potential of the PECFC, as a sustainable method for water treatment, has been demonstrated, further work is required to optimise this new technology for mineralisation of organic contaminants.

1. Introduction

Chlorophenols (CPs) are common waste water pollutants that arise mainly from the extensive use of pesticides, insecticides, bactericides, herbicides and fungicides [1,2]. Consequently, efficient and cost-effective technologies for removal of CPs from water are being investigated. Advanced oxidation processes (AOP) are amongst such technologies and involve catalytic formation of $OH^{\bullet}$ for the oxidation of organic pollutants [2–5]. Heterogeneous photocatalysis is an AOP where additional charge carriers such as holes and electrons are created in the valence and conduction bands respectively, of a semiconductor catalyst by light-induced transfer processes. To date, most studies involve the use of slurried titanium-based nanoparticles. However, practical applications are still limited by their poor activity in visible light and slow oxygen reduction reaction (ORR) at the TiO_2 surface. Due to its large band gap of *ca.* 3.2 eV [6], the photosensitivity of TiO_2 is restricted to the ultra-violet region of the light spectrum, *i.e.* $\lambda < 400$ nm, typically using only *ca.* 3% of the solar spectrum. Moreover, to separate the TiO_2 nanoparticles from the remediated water requires a post treatment filtration stage. Therefore, immobilisation of catalysts has been used in place of slurry systems to circumvent this problem. However, the disadvantages of immobilised catalysts are lower catalytic efficiencies as a result of reduced active catalyst surface area, leading to low pollutant degradation rates [7].

Several attempts to enhance the efficiency of TiO_2 catalyst using visible light has been carried out by different researchers [8–11]. Despite these efforts, the visible light activity of TiO_2-based materials is still out-performed by the photo-stable and non-toxic WO_3 photocatalyst [12,13]. With a smaller band gap of 2.5–2.8 eV [13,14] than TiO_2, its photocatalytic activity extends into the visible light region leading to utilisation of approximately 30% of solar radiation [15]. However, since the flat-band potential of WO_3 lies *ca.* 0.5 V below that of anatase TiO_2, the kinetics for the oxygen reduction process is much slower than that for TiO_2 and rather than being consumed by the ORR, the photogenerated electrons readily undergo charge recombination with the photogenerated holes in the valence band, limiting or preventing the photo-oxidation reaction. In water

* Corresponding author. Tel.: +44 01224 272941.
E-mail address: d.e.macphee@abdn.ac.uk (D.E. Macphee).

0926-3373/$ – see front matter © 2012 Elsevier B.V. All rights reserved.
http://dx.doi.org/10.1016/j.apcatb.2012.05.010

remediation, WO_3 can therefore only be used as a supported photoanode with the application of a small positive bias for removal of photogenerated electrons from the surface of the photoanode [16].

The approach of immobilising the catalyst on conducting supports and application of a polarisation potential enhances the performance of both TiO_2 and WO_3 photocatalysts [14,17]. Previously, Nissen et al. [18] carried out a study using a two compartment photochemical cell (PEC) with the WO_3 photocatalyst immobilised on a conductive glass slide as the anode, a Pt mesh as the cathode and the anode and cathode compartments separated by a 3 M KCl/agar salt bridge. The cell was operated under short circuit conditions, with the photoanode being polarised by the internal open cell potential arising from the cathode reaction in a H_2SO_4 electrolyte and the photoreaction in the anode compartment sustained without application of an external bias. The concentration decrease of 2,4-DCP was monitored over a period of 48 h and 53% degradation of the model pollutant 2,4-DCP was observed.

In this study, a photoelectrocatalytic fuel cell (PECFC) is used as an alternative reactor concept for pollutant degradation. The PECFC has a configuration that is very similar to that of a proton exchange membrane fuel cell, PEMFC. Although PEMFC's are a well-established and highly developed technology for applications mainly in micro and portable energy generation, it is a relatively new concept in photocatalysis. This technology enables the combination of photocatalytic processes with fuel cell technology where the functionality of the photocatalyst is supported by the internal fuel cell potential. Such cells have not been used yet in waste water remediation although photo-enhanced electrodes have been applied for methanol oxidation in direct methanol fuel cells [19–21]. A fuel cell configuration for the photoremediation of organic pollutants offers several advantages compared to conventional PECs.

Single-compartment phototcatalysis has the disadvantage of oxidation and reduction reactions occurring in the same liquid electrolyte and unwanted migration of charge carriers and species to either the anode or cathode may occur, compromising open circuit potential. For a more efficient photoreaction, or for reaction to occur at all, a positive bias is usually applied externally. In two-compartment cells, the use of two different electrolytes gives additional means of enhancing the potential gradient between anode and cathode therefore increasing the possibility of the open cell potential providing the driving force for the overall cell reaction. As discussed earlier, a sufficiently large open cell voltage could enable self-sustained photoelectrocatalysis. The advantages of using a PEMFC set-up for pollutant degradation are comparable to those of a two-compartment PEC, with the added benefits of a solid protonic electrolyte that allows for the use of an air-breathing cathode rather than a cathode immersed in aerated liquid. Utilising an air-breathing electrode for the concomitant oxygen reduction reaction enables a significant increase in the amount of oxygen supply available for the reduction process when compared to dissolved oxygen in an aqueous electrolyte. Furthermore, the PEMFC set-up is easier to handle in practice; it allows for simple electrode fabrication and is potentially more applicable for practical uses.

To assess the efficiency of the PECFC to remediate waste water, a commonly used CP (2,4-DCP) was used as a model pollutant. Simply monitoring the concentration of a parent compound is not always a sufficient method for assessing remediation success as intermediate degradation products with higher toxicity than the parent compound are often formed [6,22,23]. A combination of chemical and bacterial biosensor toxicity assay has therefore been used in previous studies, to concomitantly monitor degradation of organic contaminants and toxicity in aqueous solutions [18,24–27]. In this study, a bacterial biosensor (*Escherichia coli* HB101 pUCD607) toxicity assay is used in combination with chemical analysis to gain insight into changes in toxicity of the degrading parent compound. A defined level of toxicity is recorded by the biosensor to the test solution. This value, however, will be receptor (*i.e.* species—*E. coli* HB101 pUCD607) specific [28]. This genetically modified bacterial biosensor offers a rapid and convenient approach to monitor toxicity of solubilised inorganic and organic contaminants from different environmental matrices [26,28–31].

The aim of this work was to assess the efficacy of a WO_3 photocatalyst as part of the PECFC, combining visible light photocatalysis with PEMFC technology in order to enhance the AOP for remediation of 2,4-DCP. It also utilises bacterial biosensor assay to complement the standard chemical analysis.

2. Experimental

2.1. Preparation of the WO_3 photocatalyst and membrane electrode assembly (MEA)

Tungsten trioxide catalyst powder was prepared from tungsten oxide dihydrate, $WO_3{\cdot}2H_2O$ which was obtained by a precipitation reaction of sodium tungstate dihydrate, $Na_2WO_4{\cdot}2H_2O$ (99.99%, Aldrich) with HCl in aqueous solution according to Li et al. [32]. The dihydrate was subsequently heated to 550 °C in air at a heating rate of 10 °C/min. After an annealing period of 30 min, the sample was quenched to room temperature in air. For preparation of the electrode, the obtained WO_3 powder was mixed with 5% Pt on graphite carbon (Johnson Matthey, Type 286) to give a final composition of WO_3:Pt of 90:10 wt%. The electrode layer and MEA fabrication was carried out by PaxiTech Fuel Cell Systems and Technologies, Grenoble, France with the photoanode being prepared by screen-printing onto a Nafion115 membrane with a nominal thickness of 125 μm. For enhancement of current collection across the photoanode, a Teflon/carbon grid was attached to the photoanode by hot-pressing. The overall catalyst loading was 3 mg/cm^2 at the anode, with loadings of WO_3 2.7 mg/cm^2 and Pt 0.3 mg/cm^2, and the geometric electrode area was 12.5 cm^2. The cathode consisted of 40% Pt on Vulcan (Johnson Matthey) printed onto a Teflon/carbon GDL which was also attached to the Nafion membrane during the hot-pressing process. The catalyst loading at cathode was Pt 0.5 mg/cm^2.

2.2. Photoelectrocatalytic fuel cell

The schematic arrangement of the MEA in the PECFC is shown in Fig. 1 with Pt-rings as contacts (A) and the MEA consisting of five layers: gas diffusion layer (B), Nafion115 protonic membrane (C), photoanode (D), cathode layer (E) and carbon-coated Teflon current collector grid (F). The PECFC consisted of an acrylic housing with inlets and outlets for waste water or oxidant gas, and cathode and anode compartments being separated by the MEA. A quartz window allowed for illumination of the anode compartment by a Daylight^{TM} 865 bulb with wattage of 20 W and a nominal colour temperature of 6500 K for simulation of natural daylight. In the PECFC, the photo-enhanced AOP at the anode releases electrons, CO_2 and protons, as well as intermediate oxidation products. The protons are transported to the cathode through the protonic electrolyte (Nafion membrane) and the generated electrons move to the cathode *via* the external fuel cell circuit. At the cathode, the electrons take part in the ORR; oxygen from the gas phase dissociates on the platinum catalyst and is reduced (gains electron from the external circuit) to form oxide ions which react with the protons to form water. Due to the difference in potentials of the redox reactions occurring at anode and cathode, an open circuit voltage (OCV) arises. The PECFC uses the potential difference of oxidation and reduction reactions occurring at anode and cathode as a driving potential for the fuel cell reaction [33].

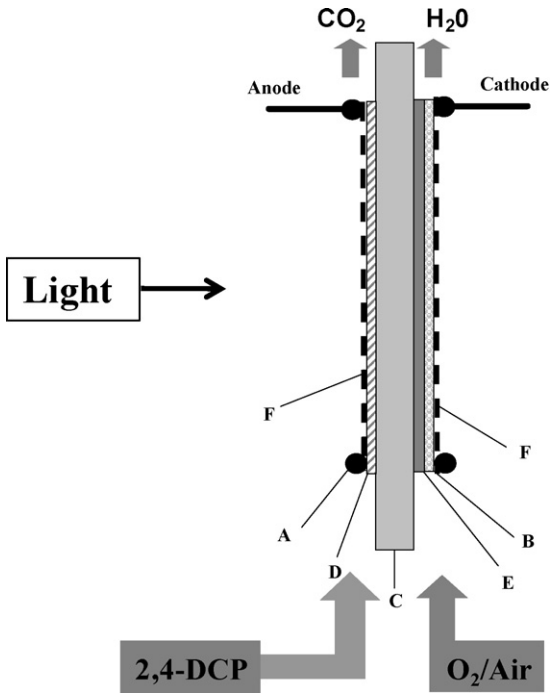

Fig. 1. Schematic detailing the arrangement of the 5-layer membrane electrode assembly (MEA) within the PECFC with components (A) Pt contacts, (B) gas diffusion layer, (C) Nafion115 membrane, (D) photoanode, (E) cathode layer and (F) carbon-coated Teflon current collector grid.

2.3. Degradation of 2,4-dichlorophenol

As the model pollutant, a 0.25 mM 2,4-DCP (99%, GC grade, Sigma–Aldrich) solution in Milli-Q water ($R > 18\,\Omega$ cm) was used in this study. An Erlenmeyer flask contained 100 ml of the 2,4-DCP solution served as a reservoir, with the reservoir solution being continuously stirred by the means of a magnetic stirrer. A silicon bung was used to seal the reservoir flask and connected with Teflon tubes to the waste water inlet and outlet of the PECFC. A continuous flow of the pollutant solution was maintained at 10 ml/min by the means of a peristaltic pump. The sample temperature was monitored continuously and maintained at $12 \pm 2\,^{\circ}$C by the means of an ice bath. An Ecochemie μ-Autolab Type III potentiostat/galvanostat was employed for measurements of the OCV at the beginning of each experiment and also for fuel cell current measurements and cell polarisation.

A set of degradation experiments was carried out under different experimental conditions (Table 1). The aim of this approach was to separate the contribution of different processes to the reduction of analyte (2,4-DCP) concentrations, *i.e.* volatilisation and adsorption, catalysis, electrocatalysis, photocatalysis and photolysis. Photoelectrocatalysis was carried out in two modes: firstly with the cell simply being short-circuited and secondly, with application of a polarisation potential of −0.5 V measured against the potential of the cathode. The value of $E_{pol} = -0.5$ V was chosen since Solarska et al. [14] found that an external bias of +0.5 V measured against NHE was optimal for methanol degradation on WO_3 photoanodes immobilised on fluoride-doped tin oxide (FTO) [14]. Each experiment was performed over a period of 24 h. In order to minimise 2,4-DCP adsorption at the cell surfaces, the cell interior was rinsed with a 0.25 mM 2,4-DCP solution for 72 h prior to the start of the runs, until the concentration of 2,4-DCP was found to remain constant and all adsorption sites were assumed to be saturated. In between runs, the cell was flushed again with a fresh solution of 0.25 mM 2,4-DCP. The surface of the catalyst was conditioned electrochemically prior to the start of each degradation run using cyclic voltammetry, with the initial potential set at the OCV of the cell and the potential being decreased by −0.5 V relative to OCV measured against the potential of the cathode at a rate of 50 mV/s in order to strip adsorbed species off the catalyst surface sites. The reverse potential was +0.2 V relative to OCV and the electrochemical cycling was carried out until the peak current was recovered, which was the case after three cycles. It was then assumed that sufficient surface conditioning had been achieved. During degradation runs, sample volumes of 500 μl were taken from the reservoir at time t_{0h} and subsequently at 1, 2, 3, 4, 5, 6 and 24 h for chemical analysis. At each time point, the pH of the solution in the reservoir was also recorded (Hanna instruments, HI 8519N). At 0, 2 and 24 h, additional samples were obtained for biosensor toxicity assays.

To assess the stability of the degradation performance, two subsequent sets of different experimental conditions were carried out sequentially and compared (giving a total of 21 runs). The reproducibility of the electrode and MEA preparation was also assessed by investigating and comparing the degradation performances of three freshly prepared MEAs under Dc and PEC* experimental conditions. A two-sample *t*-test was performed using Minitab 15 (Minitab Inc.) statistical software to check for differences between the Dc and PEC* experimental conditions.

Table 1
Photoelectrocatalytic fuel cell experimental conditions with their abbreviations.

Name	Acronym	Description
Dark control	Dc	Light off, cell open
Dark electrocatalysis (no bias)	DEC	Light off, short-circuited
Dark electrocatalysis ($E_{pol} = -0.5$ V)	DEC*	Light off, $E_{pol} = -0.5$ V
Photolysis	PL	Light on, no MEA
Photocatalysis	PC	Light on, cell open
Photoelectrocatalysis (no bias)	PEC	Light on, short-circuited
Photoelectrocatalysis ($E_{pol} = 0.5$ V)	PEC*	Light on, applied bias $E_{pol} = -0.5$ V

2.4. Chemical analysis

Time course samples were analysed by reverse phase HPLC (Thermoquest; Thermo Separation Products, San Jose, CA). The HPLC set-up consisted of a binary pump (P2000), an autosampler (AS3000), UV–vis detector (UV1000) and an integrator (SN4000) with a Pinnacle II C18 column (Thames Restek) (250 mm length; 4.6 mm i.d.; particle size of 5 μm). An isocratic mobile phase consisting of an eluent stream of 80% methanol and 20% water, flowing at a rate of 0.75 ml/min for 12 min was used. The detector wavelength was set at 230 nm and 2,4-DCP calibration standards and an internal standard (2,4-dibromophenol, 0.40 mM) were used for determination of 2,4-DCP concentrations and quality control.

Analysis of degradation intermediates was carried out using a low resolution ITMS system (Orbitrap Discovery, Thermo Instruments) coupled to a Thermo Instruments HPLC (Accela PDA detector, Accela PDA autosampler and Accela Pump). HPLC separations were carried out using an ACE 3 C18 reversed-phase column (150 mm length; 10 mm i.d.). The column temperature was maintained at 30 °C, a mobile phase of 0.5 ml/min flow rate was used and equilibrated as follows: a starting ratio of 100:0 (water:methanol) was reduced to 0:100 over 20 min. This then remained steady at this ratio for 5 min and was increased back to 100:0 (water:methanol) ratio over 25 min and then held for a further 10 min, given a total sample run time of 60 min per sample.

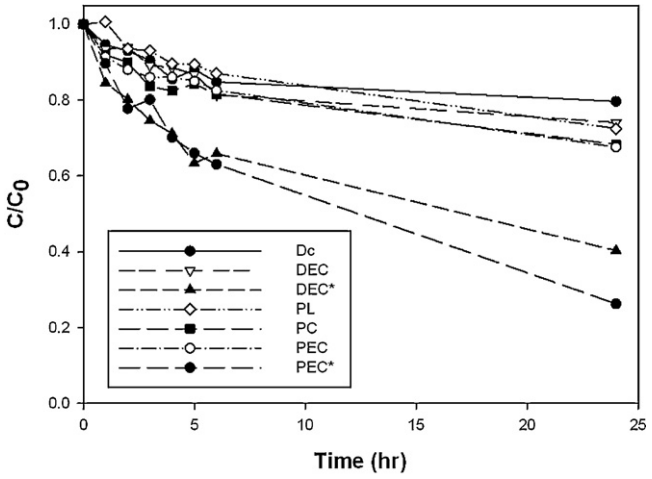

Fig. 2. Time series (24 h) indicating the residual 2,4-DCP concentration under 7 different photoelectrocatalytic fuel cell (PECFC) experimental conditions: dark control (Dc), dark electrocatalysis (DEC), dark electrocatalysis with E_{pol} = −0.5 V (DEC*), photolysis (PL), photocatalysis (PC), photoelectrocatalysis (PEC) and photoelectrocatalysis with E_{pol} = −0.5 V (PEC*).

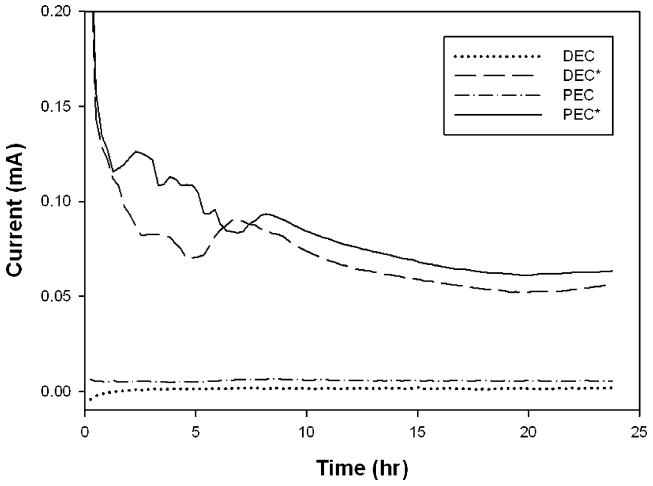

Fig. 3. Time series (24 h) indicating chronoamperometric measurements of the PECFC current during different electrocatalytic degradation runs with or without Daylight™ illumination and E_{pol} = −0.5 V.

2.5. Bacterial biosensor assay

Cultures of the biosensor (*E. coli* HB101 pUCD607) were freeze-dried using standard laboratory protocols and stored at −20 °C. Freeze-dried cells of *E. coli* were resuscitated in 10 ml 0.1 M sterile KCl solution and placed for 1 h at 25 °C on an orbital shaking incubator set at 200 rpm [29,34]. Aliquots of 100 μl resuscitated *E. coli* suspension were added at 15 s intervals to 900 μl of each sample obtained from the PECFC time course experiments. Luminescence in RLU was measured after an incubation time of 15 min using a Jade bench-top luminometer (Labtech International). The luminescence was then expressed as the percentage of a control (Milli-Q water) containing no 2,4-DCP. A high percentage luminescence relative to the control in a bioassay indicated low toxicity of the sample solution to the *E. coli* biosensor and *vice versa*.

3. Results and discussion

3.1. Degradation of 2,4-DCP

The residual 2,4-DCP concentrations measured at selected time points are shown in Fig. 2 for the different experimental conditions (Table 1). Under Dc conditions, 85% and 80% of 2,4-DCP still remained at 6 and 24 h, respectively, translating to 15% and 20% loss of 2,4-DCP. The observed 20% loss of 2,4-DCP at 24 h is most likely due to adsorption at the anode surface and volatilisation and partitioning into the headspace of the reservoir, but not to any degradation of the parent compound. Although, in principle, it could also be as a result of oxidation by the WO_3 photocatalyst, as WO_3 can exhibit redox mechanisms even in the absence of photocatalytic processes [33]. The results from the DEC, PL, PC and PEC conditions were similar to that of the Dc (81–87% and 68–74% 2,4-DCP remaining after 6 h and 24 h, respectively). This equates to 7%, 9%, 14% and 15% loss of 2,4-DCP after 24 h under DEC, PL, PC and PEC conditions, respectively (after correcting for concentration decrease under Dc). There was minimal decrease in 2,4-DCP concentration observed by these processes. However, when a polarising potential was applied to the cell, without a light source (DEC*) or with light source (PEC*), 49% and 67% degradation (after 24 h), respectively, was observed after taking into account losses attributable to Dc.

The poor performance of DEC and PEC experiments is arguably due to the small magnitude of OCV, typically around 10–40 mV. As a consequence, under open or short-circuit conditions, the anode is not sufficiently polarised in order for the electrons to be removed from its surface and for the fuel cell reaction to be sustained. Although some of the electrons are likely to be removed from the catalyst due to the internal fuel cell potential, the small OCV meant that majority of the electrons were undergoing recombination, consequently reducing the concentration of oxidative species. Previous research has shown that the WO_3 photocatalyst used in this experimental set-up is not able to spontaneously photooxidise organic species thereby resulting in recombination of photo-generated electrons and holes, if the photo-generated electrons are not removed by an external bias [16]. The reason for the small OCV could be due to fuel starvation as a result of low fuel (*i.e.* 2,4-DCP) concentration leading to O_2 cross-over from the cathode through the MEA. This results in the occurrence of a mixed anode half cell potential which increases the anode potential and hence reduced OCV. If this increased anode potential is higher than the cathode potential, a "reverse current phenomenon" could occur [35,36]. A further possibility is the adsorption of stable intermediates on the catalyst surface leading to a blockage of the active sites at the catalyst surface. These intermediate species might possess oxidation potentials which are less favourable than that of the parent compound 2,4-DCP and can only be degraded through reduction of anode potential by application of the external bias.

The fuel cell currents for the electrocatalytic and photoelectrocatalytic experiments carried out with or without application of the external bias for polarisation are shown in Fig. 3. With application of the polarisation potential of −0.5 V relative to OCV (DEC* and PEC*) experiments, fuel cell currents of around 130 μA were measured after 1 h. The cell current was found to have decreased by *ca.* 50% to a value of 60 μA by the end of the experiment. The current trace for the PEC* experiment shows several broad current maxima appearing within the first 8 h of the run. Daylight™ illumination enhanced the cell current, particularly within the first 3 h of the experiment. For the short-circuited fuel cell experiments without application of external bias (DEC and PEC), the observed currents were, however, very small, with magnitudes of below 1 μA/cm^2 and even reversed under DEC experimental conditions. The reversed current phenomenon is probably due to an increase of the potential at the anode. Data show that a higher current was generated in both PEC* and DEC*, than for PEC and DEC experimental conditions, which is

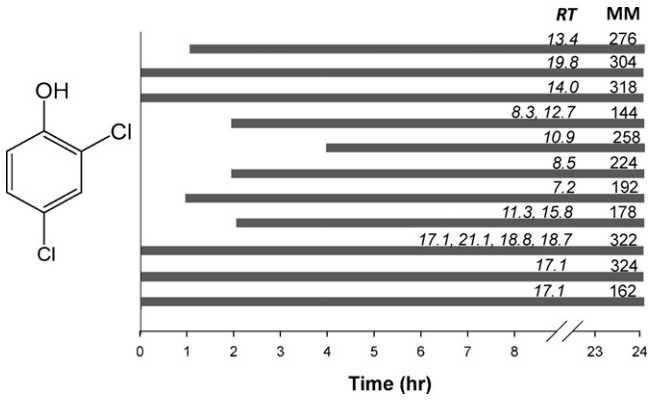

Fig. 4. Schematic detailing a summary of molecular masses (MM) and retention times (RT) of 2,4-DCP degradation intermediate products and time of appearance of the products over a degradation time of 24 h.

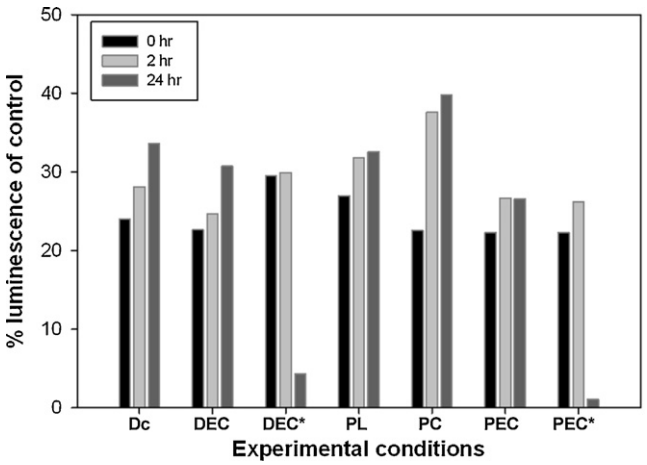

Fig. 5. Percentage luminescence from *E. coli* HB101 pUCD607 biosensor toxicity assays for 0, 2 and 24 h under 7 different photoelectrocatalytic fuel cell (PECFC) experimental conditions: dark control (Dc), dark electrocatalysis (DEC), dark electrocatalysis with $E_{pol} = -0.5$ V (DEC*), photolysis (PL), photocatalysis (PC), photoelectrocatalysis (PEC) and photoelectrocatalysis with $E_{pol} = -0.5$ V (PEC*).

complementary to the results obtained from chemical analysis for the degradation rates.

3.2. Degradation intermediates

Photocatalytic degradation reactions involve the formation and participation of free radical species in on-going catalytic processes. This makes identification of oxidative degradation pathways and degradation intermediates particularly challenging. Combined HPLC–MS data provided information on the molecular masses of degradation products being formed during the remediation process. The different molecular masses and retention times observed for these compounds are summarised in Fig. 4. A molecular mass of around 144 or 178 could be indicative of dichlorinated benzoquinone or catechol as possible degradation intermediates [37,38]. The species with molecular masses of 304, 318, 322 and 324 were already present at the first sampling time, as a result of dimerisation of the 2,4-DCP molecule possibly occurring *via* a free radical reaction mechanism. The observed variation in peak area of these species indicated that the largest concentration of this compound was present during the first few hours of the experimental runs. Interestingly, the presence of dimerisation products was consistent with the occurrence of the current maxima observed in the 2,4-DCP concentration profile at 2–5 h (Fig. 3). Furthermore, an overall decrease in retention times was observed with time of exposure in the cell. This is associated with an increase in hydrophilicity, consistent with continuing oxidation processes. This increased hydrophilicity, due to increased polarity in the functional groups on ring structures or to ring opening, represents a shift towards molecules which are more amenable to further oxidation and complete mineralisation.

The HPLC–MS results are only preliminary at this point and a much more extensive study of the intermediates is needed in order to conclude on degradation mechanisms.

3.3. E. coli HB101 pUCD607 biosensor toxicity assay

The toxicity response at time 0 h for samples in all seven experimental conditions was *ca.* 25–30% luminescence of control. The low luminescence relative to the control is due to the toxic effect of 2,4-DCP and agrees with previous studies where a lower concentration of 2,4-DCP (0.20 mM) still caused a 50% decrease in luminescence [18]. At $t = 2$ h, an increase in luminescence was observed under all experimental conditions, correlating to the reduction of 2,4-DCP concentration through different processes. At 24 h, however, substantial differences for the different experimental conditions became apparent. Under experimental conditions where no polarisation potential of −0.5 V was applied (DEC, PL, PC and PEC), the percentage luminescence continued to increase concomitant with the continued losses of 2,4-DCP, indicating decreasing toxicity (Fig. 5). However, when the cell was polarised by −0.5 V during DEC* and PEC* runs, the luminescence was found to be reduced to 4.32% and 1.08% at 24 h for DEC* and PEC*, respectively (Fig. 5). The reduction in luminescence indicated an increased toxicity effect despite these 2 experimental conditions having the largest concentration decrease of 2,4-DCP (Fig. 2). This change in toxicity effects between 2 h and 24 h could be attributed to formation of more and/or less toxic degradation intermediates resulting in a multi-component solution of parent compound 2,4-DCP and a number of different degradation intermediates whose toxicity may have additive, antagonistic or synergistic effects on the biosensor, depending on their concentrations [25].

The monitored pH values under the seven different experimental conditions showed that there was a reduction in pH of *ca.* 1.5 pH units ($t_0 = 5.5$–6.0, $t_{24\,h} = 4.0$–4.8). This observed reduction in pH is not likely to cause the reduction in luminescence of the biosensor under DEC* and PEC* conditions as the *lux*-marked biosensor used in this study has previously been shown to be consistent across a pH range of 4.0–6.5 [39]. A decrease of pH however, could suggest that oxidative degradation is occurring, as proton generation is a consequence of stepwise electron withdrawal.

3.4. Stability and reproducibility of the PECFC degradation performance

The stability of the degradation performance of the PECFC was investigated over a period of 24 h by carrying out three sequential runs using the same MEA under similar experimental conditions. Whilst Dc, DEC, PL, PC and PEC remained relatively constant across the three sequential runs, DEC* and PEC* showed considerable variations. As an example, Fig. 6a and b shows the three sequential 2,4-DCP degradation plots and associated fuel cell currents during the PEC* experiment. A continuous decrease in remediation capability occurred from the first to the last sequential run, with the final PEC*-c run differing only marginally from the measured values during the Dc run (Fig. 6a), indicating loss of catalytic activity. This could be due to the delamination of the carbon current collector grid and the gas diffusion layer at the cathode as a possible consequence of electrode corrosion, leading to a decrease of active electrode area and poor stability [40]. Other potential reasons for

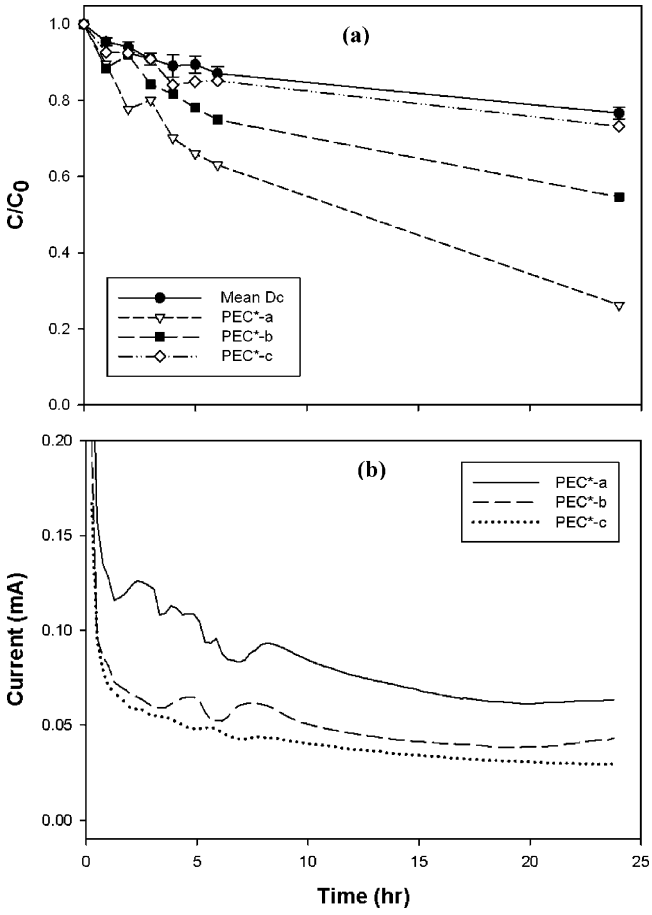

Fig. 6. Individual time series (24 h) indicating (a) residual 2,4-DCP concentration under photoelectrocatalysis with $E_{pol} = -0.5$ (PEC*) experimental conditions in comparison with the dark control (Dc) and (b) corresponding chronoamperometric measurements of the PECFC.

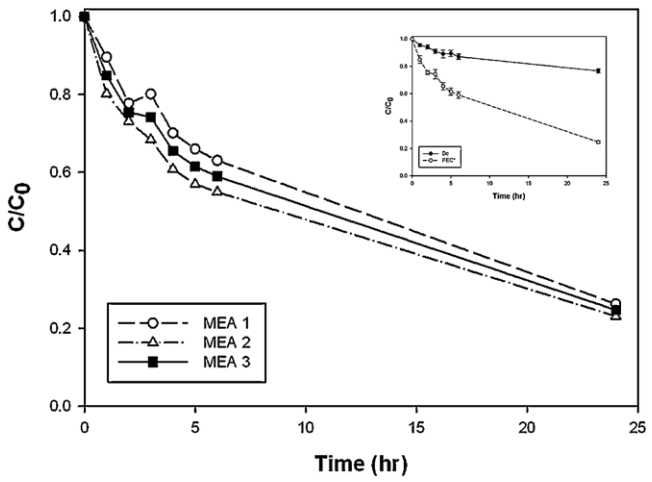

Fig. 7. Individual time series (24 h) indicating residual 2,4-DCP concentrations in the photoelectrocatalytic fuel cell (PECFC), on successive 24 h catalytic exposures photoelectrocatalysis with $E_{pol} = -0.5$ V (PEC*) using 3 different MEAs in comparison with the dark control (Dc). Vertical bars (insert) represent standard errors of the means of 3 replicates (MEA-1, MEA-2 and MEA-3).

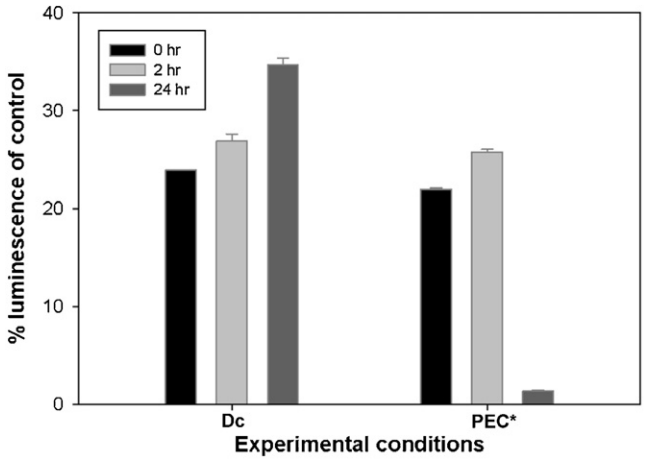

Fig. 8. Percentage luminescence from *E. coli* HB101 pUCD607 biosensor toxicity assays for 0, 2 and 24 h under 2 photoelectrocatalytic fuel cell (PECFC) experimental conditions: dark control (Dc) and photoelectrocatalysis with $E_{pol} = -0.5$ V (PEC*). Values represent means (±std err) of 3 replicates (MEA-1, MEA-2 and MEA-3).

the loss of efficiency of the PECFC are firstly, MEA degradation as a result of carbon or catalyst corrosion which leads to agglomeration of nanoparticles and loss of the catalyst (WO_3) from the electrode surface [35]. Secondly, an increase of internal cell resistances through processes such as degradation of the Nafion membrane is also possible, since fuel cell currents were observed to decrease rather than increase for the sequential runs which were measured at the same polarisation potential of −0.5 V. Thirdly, a further possibility could be the build up of 2,4-DCP and degradation products on the surface of the catalyst between sequential runs which had not been completely stripped off by electrochemical oxidation during electrode conditioning.

In addition, the corresponding biosensor response of the individual sequential runs of PEC* (Fig. 6b) also showed a significant variation between the three runs. At $t = 24$ h there was a steady increase in luminescence of the biosensor corresponding to more 2,4-DCP remaining from the first to the last sequential run (PEC*-a to PEC*-c) compared with the 3 sequential Dc runs, which showed minimal difference from PEC*-a" to PEC*-c. As the chemical analysis showed that the optimum performance of the PECFC occurred in PEC*-a, it can be inferred that 2,4-DCP degradation occurred the most and therefore this first run has the greatest potential for the formation of intermediates which could be more toxic. This sample had the lowest luminescence relative to the control (1.08%). Therefore, the biosensor responses suggested the steady increase in luminescence in sequential samples was due to less formation of degradative intermediate compounds that were more toxic than the parent compound (data not shown). Many potential 2,4-DCP intermediates have indicated greater toxicity than 2,4-DCP [18,38].

In a further set of PEC* degradation experiments, the reproducibility of the electrode and MEA synthesis as well as the experimental method for remediation studies was assessed. Here 3 different runs were carried out using a freshly prepared and conditioned MEA (Fig. 7). All three experiments showed similar degradation rates in both Dc and PEC* experimental conditions over a period of 24 h. There was a significant difference in PECFC degradation performance between Dc and PEC* (Fig. 7 insert) experimental conditions ($p < 0.05$). Reproducibility was further assessed by a biosensor toxicity assay for both Dc and PEC* runs. The result of the biosensor toxicity assay (Fig. 8) again confirms the reproducibility of the MEA as all three MEAs give very similar biosensor responses depicting an increased toxicity effect as intermediate products are being formed during the PEC* run.

4. Conclusions

The concept of the PECFC with a cell configuration based on PEMFC technology has been applied for the first time for the

purpose of 2,4-DCP degradation. Successful visible light-enhanced degradation occurred when the cell was polarised by −0.5 V (PEC*), resulting in a 74% decrease in concentration of a highly persistent chlorinated phenol, 2,4-dichlorophenol, over a period of 24 h from which over 54% were indeed accountable to the degradation process. The performance of the PECFC was significantly limited by the small OCV of the cell in the experimental conditions without application of a polarisation potential. Moreover, there was an observed loss of efficiency of the PECFC with prolonged use of a single MEA. Degradation experiments carried out with 3 different MEAs showed reproducibility of degradation performance across MEAs made to the same specifications.

The combination of chemical and bacterial biosensor toxicity assessments for the monitoring of 2,4-DCP degradation during remediation has proven to be a valuable amalgamation of analytical techniques. Although 2,4-DCP was degraded, analyses indicated the formation of intermediate degradation products during the remediation process that were of higher toxicity than the parent compound. The potential of the PECFC as a sustainable method for water treatment has been successfully demonstrated, however, further work is required to optimise the different cell and system components and to further develop this new technology for mineralisation of organic contaminants.

Acknowledgements

The authors would like to thank Glasgow City Council for funding this work. We would also like to thank Dr. Eric Lachowski for the SEM work, Dr. Sian Masson for the CV measurement on WO_3 electrodes and Dr. Renaut and Annette Mosdale from PaxiTech for the MEA preparation and all their valuable advice.

References

[1] M. Czaplicka, Science of the Total Environment 322 (2004) 21–39.
[2] M. Pera-Titus, V. García-Molina, M.A. Banõs, J. Giménez, S. Esplugas, Applied Catalysis B 47 (2004) 219–256.
[3] W.H. Glaze, Chemical Oxidation 3 (1994) 44–57.
[4] S. Esplugas, J. Giménez, S. Contreras, E. Pascual, M. Rodríguez, Water Research 36 (2002) 1034–1042.
[5] B. Bayarri, O. González, M.I. Maldonado, J. Giménez, S. Esplugas, Journal of Solar Energy, Transactions of ASME 129 (2007) 61–66.
[6] A. Mills, S. Morris, R. Davies, Journal of Photochemistry and Photobiology A 70 (1993) 183–191.
[7] D.F. Ollis, E. Pelizzetti, N. Sperone, Heterogeneous photocatalysis in the environment: application to water purification, in: N. Sperone, E. Pelizzetti (Eds.), Photocatalysis—Fundamentals and Applications, Wiley, Chichester, 1989, p. 603.
[8] W.Y. Choi, A. Termin, M.R. Hoffmann, Journal of Physical Chemistry 98 (1994) 13669–13679.
[9] R. Asahi, T. Morikawa, T. Ohwaki, K. Aoki, Y. Taga, Science 293 (2001) 269–271.
[10] H. Wang, J.P. Lewis, Journal of Physics: Condensed Matter 17 (2005) L209–L213.
[11] C. Di Valentin, G. Pacchioni, A. Selloni, Chemistry of Materials 17 (2005) 6656–6665.
[12] M. Hepel, J. Luo, Electrochimica Acta 47 (2001) 729–740.
[13] C.J. Sartoretti, B.D. Alexander, R. Solarska, I.A. Rutkowska, J. Augustynski, Journal of Physical Chemistry B 109 (2005) 13685–13692.
[14] R. Solarska, C. Santato, C. Jorand-Sartoretti, M. Ulmann, J. Augustynski, Journal of Applied Electrochemistry 35 (2005) 715–721.
[15] C. Santato, M. Odziemkowski, M. Ulmann, J. Augustynski, Journal of the American Chemical Society 123 (2001) 10639–10649.
[16] C. Santato, M. Ulmann, J. Augustynski, Journal of Physical Chemistry B 105 (2001) 936–940.
[17] Neumann-Spallart, Chimia 61 (2007) 806–809.
[18] S. Nissen, B.D. Alexander, D. Ilyas, M. Tillotson, R.P.K. Wells, D.E. Macphee, K. Killham, Environmental Pollution 157 (2009) 72–76.
[19] K. Drew, G. Girishkumar, K. Vinodgopal, P.V. Kamat, Journal of Physical Chemistry B 109 (2005) 11851–11857.
[20] K.-W. Park, S.-B. Han, J.-M. Lee, Electrochemistry Communications 9 (2007) 1578–1581.
[21] C. Jia, H. Yin, H. Ma, R. Wang, X. Ge, A. Zhou, X. Xu, Y. Ding, Journal of Physical Chemistry 113 (2009) 16138.
[22] A.J. Hoffman, G. Mills, H. Yee, M.R. Hoffmann, Journal of Physical Chemistry 96 (1992) 5546–5552.
[23] H. Zhao, D. Jiang, S. Zhang, K.W. Wen, Journal of Catalysis 250 (2007) 102–109.
[24] M.P. Ormad, J.L. Ovelleiro, Kiwi, Applied Catalysis B 32 (2001) 157–166.
[25] T. Tiensing, N. Strachan, G.I. Paton, Journal of Environmental Monitoring 4 (2002) 482–489.
[26] D. Trott, J.J.C. Dawson, K.S. Killham, Md. R.U. Miah, M.J. Wilson, G.I. Paton, Journal of Environmental Monitoring 9 (2007) 44–50.
[27] J.J.C. Dawson, C.O. Iroegbu, H. Maciel, G.I. Paton, Journal of Applied Microbiology 104 (2008) 141–151.
[28] J.J.C. Dawson, C.D. Campbell, W. Towers, C.M. Cameron, G.I. Paton, Environmental Pollution 142 (2006) 493–500.
[29] S. Sousa, C. Duffy, H. Weitz, L.A. Glover, E. Bar, R. Henkler, K. Killham, Environmental Toxicology and Chemistry 17 (1998) 1039–1045.
[30] S. Rodriguez-Mozaz, M.P. Marco, M.J. Lopez de Alda, D. Barcelo, Pure and Applied Chemistry 76 (2004) 723–752.
[31] S. Girotti, E.N. Ferri, M.G. Fumo, E. Maiolini, Analytica Chimica Acta 608 (2008) 2–29.
[32] Y.M. Li, M. Hibino, M. Miyayania, T. Kudo, Solid State Ionics 134 (2000) 271–279.
[33] D.E. Macphee, D. Rosenberg, M.G. Skellern, R.P. Wells, J.A. Duffy, K.S. Killham, Journal of Solid State Electrochemistry 15 (2011) 99–103.
[34] E.A.S. Rattray, J.I. Prosser, K. Killham, L.A. Glover, Applied and Environment Microbiology 56 (1990) 3368–3374.
[35] Y. Shao, G. Yin, Y. Gao, Journal of Power Sources 171 (2007) 558–566.
[36] S. Von Dahlen, G.G. Scherer, A. Wokaun, I.A. Schneider, ECS Transactions 33 (2010) 1365–1374.
[37] M. Czaplicka, Journal of Hazardous Materials 134 (2006) 45–59.
[38] E. Moctezuma, B. Zermeño, E. Zarazua, L.M. Torres-Martínez, R. García, Topics in Catalysis 54 (2011) 496–503.
[39] G.M. Sinclair, G.I. Paton, A.A. Meharg, K. Killham, FEMS Microbiology Letters 174 (1999) 273–278.
[40] Z. Qi, H. Tang, Q. Guo, B. Du, Journal of Power Sources 161 (2006) 864–871.